# Polaron and bipolaron formation in a cubic perovskite lattice

Vladimir N. Kostur and Philip B. Allen
*Department of Physics, State University of New York, Stony Brook, New York 11794-3800*
(Received 8 August 1996; revised manuscript received 25 November 1996)

The Rice-Sneddon model for $BaBiO_3$ offers a starting point for discussing polarons and bipolarons in a three-dimensional oxide crystal. We use exact diagonalization methods on finite samples to study the stability and properties of polarons and bipolarons. Because polarons, when they form, turn out to be very well localized, we are able to converge accurately our calculations for two-electron bipolaron wave functions, accounting for the Coulomb interaction without approximation. Some of our results are compared with and interpreted by reference to the variational method of Landau and Pekar. We calculate both electronic and vibrational excitations of the small polaron solutions, finding a single vibrational state localized with the full symmetry of the polaron, which has its energy significantly decreased at the onset of polaron formation. Both on-site (Hubbard) and long-range Coulomb repulsion are included in the bipolaron calculation, but due to the high degree of localization, the long-range part has only a small influence. For a reasonable on-site repulsion $U$ equal to two times the band width $W$, bipolaron formation is significantly suppressed; there is a large window of electron-phonon coupling where the polaron is stable but the bipolaron decays into two polarons. [S0163-1829(97)04230-6]

## I. INTRODUCTION

The electron localized on an ion (or a few ions) can cause displacements of neighboring ions from their positions in the crystal lattice. The quasiparticle formed by an electron and corresponding lattice displacements is called a *polaron*.[1–5] The polaron is a *small polaron* if the electron is localized mostly on one ion (more than 50%) or an *intermediate polaron* if localized on a group of ions. We reserve the term *large polaron* for a delocalized polaron which is an electron moving together with polarization of the surrounding medium. It is possible that the surrounding ions ''overscreen'' the negative charge of the localized electron and attract another electron to the same site. Two electrons bound in such way form a *bipolaron*.[2,6] The important issue for bipolaron formation is a quantitative analysis of the relative strength of the electron-lattice interaction responsible for two electrons being coupled and the electron-electron (Coulomb) forces which try to break the bipolaron apart. If the Coulomb repulsion between electrons exceeds some critical value the bipolaron is less stable than two separated polarons.

Theoretical interest in perovskites continues due to the variety of interesting physical properties exhibited by these compounds. The ideal structure of $ABX_3$ perovskite is cubic (Fig. 1) with cation $B$ surrounded by six anions $X$. Localization of an electron on cation $B$ causes the anions to move away from $B$.[7] The displacements of anions decrease the total energy of the system and can result in self-trapping the electron on the site $B$. A model describing such processes must take into account which $B$-atom orbitals are occupied, the electron-lattice coupling, and the electron-electron correlations.

In the present paper we study polaron and bipolaron formation in a model originally proposed by Rice and Sneddon[8] for doped $BaBiO_3$, such as $Ba_{1-x}K_xBiO_3$ (BKBO). These materials are nearly cubic perovskites, with a fairly simple set of valence electron states, exhibiting superconducting transition temperatures as high as 32 K at optimal doping. The oxygen atoms are relatively easy to move and polaron formation is mainly caused by the displacements of these ions. We choose this model both because of its relation to physically important materials ($SrTiO_3$ and $WO_3$ could be studied by a closely related model with $T_{2g}$ $d$ states instead of $s$-electron states[9]) and also because it makes a nice test model for looking at the criteria for polaron formation and the properties of polarons on a three-dimensional (3D) microscopic basis. In this study, for simplicity, we consider the hypothetical case of an almost empty band, corresponding to $KBiO_3$, or BKBO with $x=1$.

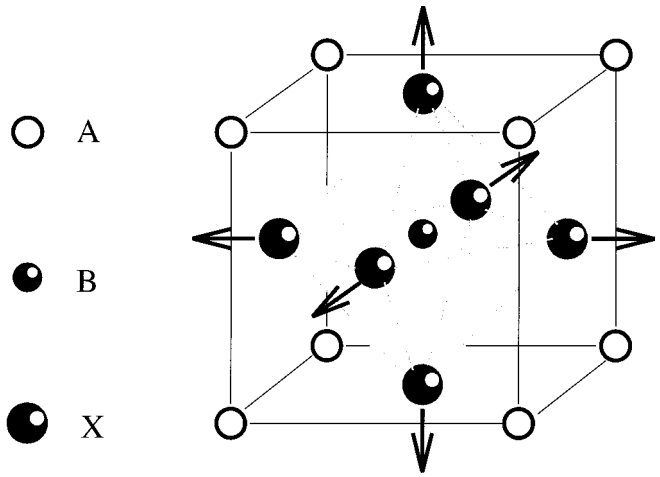


FIG. 1. The ideal structure of an $ABX_3$ perovskite. ($A$ is a larger cation, $B$ is a smaller cation, and $X$ is an anion.) The larger cation $A$ has usually smaller positive charge than cation $B$. The substitution of $A$ by another ion $A'$ with valence different from $A$ changes the number of carriers in the system. If the carrier is localized on cation $B$, Coulomb forces cause the anions $X$ to be displaced away from $B$.

 

Our principal results are (1) there is a sudden jump at a critical coupling strength from a large (delocalized) polaron to a very small, well-localized polaron with radius smaller than interionic distance. There is no self-localized solution with larger polaron radius. This agrees with the results of Toyozawa[10] and with the general classification of Emin and Holstein.[11] (2) The bipolaron breaks apart even at moderate strength of on-site Coulomb repulsion and (3) small polaron formation is accompanied by a characteristic formation of localized vibrations of shifted energy which may serve as a good experimental signature.

## II. MODEL HAMILTONIAN

The generic Hamiltonian is

$$H=H_0+H_C=H_t+H_{e\text{-ph}}+H_{\text{ph}}+H_C, \tag{1}$$

where $H_t$, $H_{e\text{-ph}}$, $H_{\text{ph}}$, and $H_C$ are , correspondingly, hopping, electron-phonon, phonon, and Coulomb terms. With the BKBO system in mind we use for the hopping term, only one bismuth $s$ orbital per cell with hopping only to nearest bismuth neighbors:

$$H_t=-t\sum_{\langle i,j\rangle\sigma}\hat{c}^{\dagger}_{i\sigma}\hat{c}_{j\sigma}. \tag{2}$$

This has the usual cosine dispersion relation with bandwidth $W$ equal to $12t$. We take the value of $t$ to be 200 meV following band-structure calculations.[12] The effective mass $m^*$ is 1.04 of bare electron mass at the $\mathbf{k}=0$ band minimum, using the lattice parameter $a=4.28$ Å of $BaBiO_3$. We assume that the same model for electrons in BKBO can be applied to all the region of K concentration, because the antibonding Bi($6s$)-O($2p$) conduction band in cubic BKBO is minimally affected by substitutional K doping at the Ba sites.[12] First-principles linear muffin-tin orbital calculations for different phases of BKBO: $KBiO_3$, $K_{0.5}Ba_{0.5}BiO_3$, and $BaBiO_3$ reveal a single band near Fermi energy to be largely independent on potassium doping.[13]

Hypothetical $KBiO_3$ in this model has no electrons. Each Bi atom is in the 5+ ionization state with no remaining valence electrons, whereas $BaBiO_3$ in this model has a half-filled band of $Bi^{4+}$ ions. Real $BaBiO_3$ is insulating, and is most simply understood as having alternating $Bi^{3+}$ and $Bi^{5+}$ ions. The $Bi^{3+}$ ions have two valence electrons bound to them, and repel the surrounding six oxygen atoms, which are attracted to the more positive $Bi^{5+}$ ions.[7] The important lattice degree of freedom is therefore the motion of $O^{2-}$ ions along the direction of the Bi-O bonds. Such displacements couple strongly to the Bi $6s$ electron states. The Rice-Sneddon model (RSM) incorporates this coupling through the terms

$$H_{e\text{-ph}}=\frac{g}{a}\sum_{i\sigma}\sum_{\alpha=1}^{3}[u_{i-,\alpha}-u_{i+,\alpha}]\hat{c}^{\dagger}_{i\sigma}\hat{c}_{i\sigma}, \tag{3}$$

$$H_{\text{ph}}=\sum_i\sum_{\alpha=1}^{3}\left[\frac{P^2_{i,\alpha}}{2M}+\frac{1}{2}M\omega_0^2u^2_{i,\alpha}\right]. \tag{4}$$

The notation $u_{i,\alpha}$ refers to the displacement of the oxygen atom (labeled by $\{i,\alpha\}$) which neighbors the $i$th Bi atom in the $\alpha=x,y,z$ Cartesian direction. Only displacements in the direction $\hat{\alpha}$ of the bond are considered, because these are expected to dominate the physics of polaron formation (see Fig. 2). The notation $u_{i+,\alpha}$ means exactly the same as $u_{i,\alpha}$, whereas $u_{i-,\alpha}$ refers to the displacement of the oxygen atom which neighbors the $i$th Bi atom in the $\alpha=-x,-y,-z$ Cartesian direction. The atoms labeled by $(i-,\alpha)$ can also be labeled in the form $(i',\alpha)$ by reference to the appropriate nearby Bi atom $i'$. The coupling constant $g$ will be treated as a fitting parameter. Its determination requires more detailed information about the electron-lattice interaction for the particular cubic perovskite structure (see Sec. III). Equation (3) contains the effect that an ''inhaling'' of the negative oxygen ions around a central Bi ion will raise the on-site energy of the bismuth $s$ orbital, by an amount equal to $g$ per fractional displacement $u/a$ of each of the six surrounding atoms. However, this costs elastic energy as given in Eq. (4). We take $M$ as the oxygen atomic mass, and $\omega_0$ to have the value 42 meV of a typical oxygen bond-stretching vibration.[14] (It corresponds to spring energy $M\omega_0^2a^2/2$ being $\approx 62$ eV.) Various values of $g$ will be used, in the physically expected range of 4–12 eV. Finally, there is a Coulomb interaction between electrons,

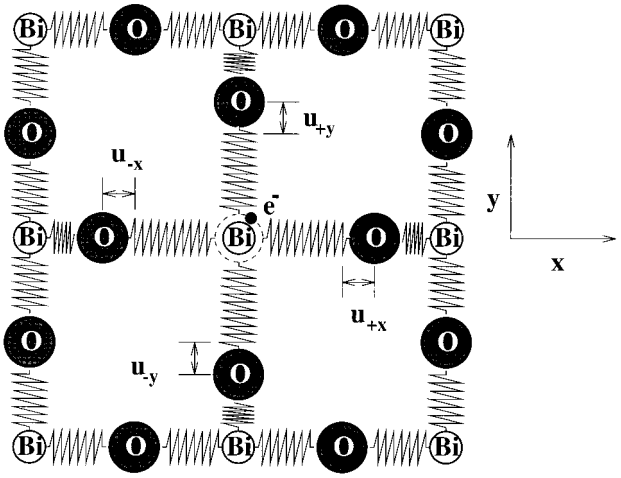


FIG. 2. The displacements of oxygen along Bi-O bonds in the $XY$ plane when an electron is localized on the Bi ion. The changes in total energy are proportional to displacements if the displacements are small. Only the nearest ions displacements are shown for simplicity.

$$H_C=U\sum_i\hat{n}_{i\uparrow}\hat{n}_{i\downarrow}+\sum_{i\neq j,\sigma\sigma'}\frac{e^2}{\varepsilon|r_i-r_j|}\hat{n}_{i\sigma}\hat{n}_{j\sigma'}. \tag{5}$$

Various values of $U$ comparable with $W=12t$ will be used for the on-site (Hubbard) term in the Coulomb interaction, and the value $\varepsilon=5$ will characterize the long-range Coulomb repulsion.

The vacuum of this model corresponds to $KBiO_3$, with no electrons, and only zero-point vibrational energy $3N\hbar\omega_0/2$. We will see that shifts of the zero point energy are not very important, so we can ignore this term and define the vacuum as having energy zero. For the half-filled case, the ground state (for not too strong Coulomb repulsion compared to electron-phonon coupling) has a period-doubling distortion

of the oxygens. Alternate bismuth sites have the oxygens ''breathing'' either in or out, and electron charge either diminished or increased from the average of one electron per site. This corresponds to the experimental insulating state of $BaBiO_3$, and gives a new vacuum into which carriers can be introduced by doping. Neglecting Coulomb repulsion, this regime was studied numerically by Yu *et al.*,[15] who found, in agreement with experiment, that the insulating gap persisted for a wide range of K doping. In $d=2$, this model with application to $CuO_2$ planes of high-$T_c$ superconductors was studied by Prelovšek *et al.*[16] They use an adiabatic treatment of the phonon degrees of freedom and the Hartree approximation for the Hubbard term. Most of the physics in the model turns out to be determined by two dimensionless parameters, $U/W=U/12t$ governing the Coulomb repulsion, and a parameter $\Gamma$, of size $\approx 1$, defined as

$$\Gamma = g^2/M\omega_0^2 a^2 t, \tag{6}$$

which governs electron-phonon effects. It is convenient to use as the unit of energy, the hopping parameter $t$, and to use a scaled Hamiltonian $\tilde{H}=H/t$. The convenient unit of length is $u_0=\sqrt{t/M\omega_0^2}$, and we define scaled lattice displacements $\tilde{u}_{i,\alpha}=u_{i,\alpha}/u_0$ and momenta $\tilde{P}_{i,\alpha}=u_0 P_{i,\alpha}/\hbar$. Then the scaled Hamiltonian is

$$\tilde{H}_0 = -\sum_{i\sigma} c_{i\sigma}^{\dagger} c_{i\sigma} + \sqrt{\Gamma}\sum_{i\sigma\alpha} [\tilde{u}_{i-,\alpha} - \tilde{u}_{i+,\alpha}] c_{i\sigma}^{\dagger} c_{i\sigma} + \frac{1}{2}\sum_{i\alpha}\left[\tilde{u}_{i,\alpha}^2 + \left(\frac{\hbar\omega_0}{t}\right)^2 \tilde{P}_{i,\alpha}^2\right]. \tag{7}$$

We see from Eq. (7) that a third dimensionless parameter is $\hbar\omega_0/t$. This governs the size of nonadiabatic effects. We will show that such corrections are small in our model.

## III. POLARON

Our only approximation (apart from finite size errors which are well controlled) is the Born-Oppenheimer (adiabatic) treatment of the vibrations. Inserting one electron into the empty-band vacuum, and letting the oxygen atoms have some fixed distortion pattern $\{u\}$, we look for the lowest energy one-electron state with wave function

$$\psi_{\uparrow}(\{u\}) = \sum_i a_i(\{u\}) c_{i,\uparrow}^{\dagger} |\text{vac}\rangle, \tag{8}$$

where $a_i(\{u\})$ are the site amplitudes of the electron wave function. Later the dependence of $a_i$, etc., on the parameters $\{u\}$ will be implicit and not explicitly designated. This electron state has energy $\epsilon_0(\{u\})$, measured relative to the bottom of the band $\epsilon_0(\{0\})$. The total energy is this plus the elastic energy $\langle H_{\text{ph}}(\{u\})\rangle$. Then we vary the displacements $\{u\}$ looking for the absolute minimum total energy. If the coupling constant $\Gamma$ is small, the minimum occurs at $\{u\}=\{0\}$ and has total energy 0. This corresponds to a large polaron solution, which in adiabatic approximation is just an electron in the bottom of the band of the undeformed crystal. If we were to include the nonadiabatic coupling of this electron with virtual phonons, there would be an alteration of the mass and energy of this electron. Specifically, the energy shift would be

$$\Delta\epsilon_0 = \sum_{j,k} \frac{|M_{0j}^k|^2}{\epsilon_0 - \epsilon_j - \hbar\omega_k} \tag{9}$$

in terms of the one electron energies $\epsilon_j$ and the phonon energies $\hbar\omega_k$ of the unperturbed band. This sum can be evaluated as follows:

$$\frac{\Delta\epsilon_0}{t} = 2\Gamma\left(\frac{\hbar\omega_0}{4t}\right)\left[1 - S\left(\frac{\hbar\omega_0}{4t}\right)\right], \tag{10}$$

$$S(x) = \frac{1}{N}\sum_{\mathbf{Q}} \frac{x}{x + f(\mathbf{Q})}, \tag{11}$$

$$f(\mathbf{Q}) = \sin^2\left(\frac{Q_x a}{2}\right) + \sin^2\left(\frac{Q_y a}{2}\right) + \sin^2\left(\frac{Q_z a}{2}\right). \tag{12}$$

For our choices of $\omega_0$ and $t$, the ratio $\hbar\omega_0/4t$ is 0.053 and the sum $S$ in Eq. (11) is 0.12. Thus the self-energy shift of the large polaron is $\approx 0.09\Gamma$ which turns out to be small compared to the energies that we will find for the small polaron regime. This is shown later in Fig. 6. Thus we can safely ignore the nonadiabatic effects. By a similar argument (which we will explain in more detail later) the zero-point contribution to the elastic energy can be ignored, and the elastic contribution to the small polaron energy is just the second term of Eq. (4).

To evaluate the one-electron energy $\epsilon_0(\{u\})$ for the distorted lattice requires a finite size system, which we choose to be an orthorhombic cell (our ''supercell'') with $N=N_1\times N_2\times N_3$ Bi atoms on a cubic lattice, and $3N$ oxygens on the Bi-Bi bonds, and periodic boundary conditions. The Lanczos technique[17] was used for finding the ground-state energy and a few lowest excited states of the Hamiltonian (1), and conjugate gradient minimization was used to find the optimum values of the oxygen displacements $\{u\}$. Results are shown in Fig. 3. Beyond a critical value $\Gamma_P = 1.96$ it becomes favorable for oxygens to distort and form a localized small polaron state. We define the location $\vec{r}_0$ and radius $r_P$ of the polaron by

$$\vec{r}_0 = \sum_i |a_i|^2 \vec{r}_i, \tag{13}$$

$$r_P^2 = \sum_i |a_i|^2 (\vec{r}_i - \vec{r}_0)^2. \tag{14}$$

The typical oxygen displacements near $\vec{r}_0$ are $u_0 \approx 0.03\ a$, and they decay exponentially far from $\vec{r}_0$.

The radius of the polaron at the transition is 0.49 in units of Bi-Bi distance, that is, it is very well-localized with 90% of the electron density concentrated on one site. As $\Gamma$ increases beyond the critical value, the radius further shrinks, and the binding energy rapidly increases to values of order $t$ and bigger. Our results are plotted in Fig. 3. For $\Gamma$ less than the critical value, the radius is shown as a finite number $\approx 4a$ reflecting the finite size of the cell; the actual radius is infinite. For values of $\Gamma$ slightly less than critical, our minimization procedure locates a metastable small polaron solution with a small positive energy, which is shown in Fig. 3 as a small hysteretic region.

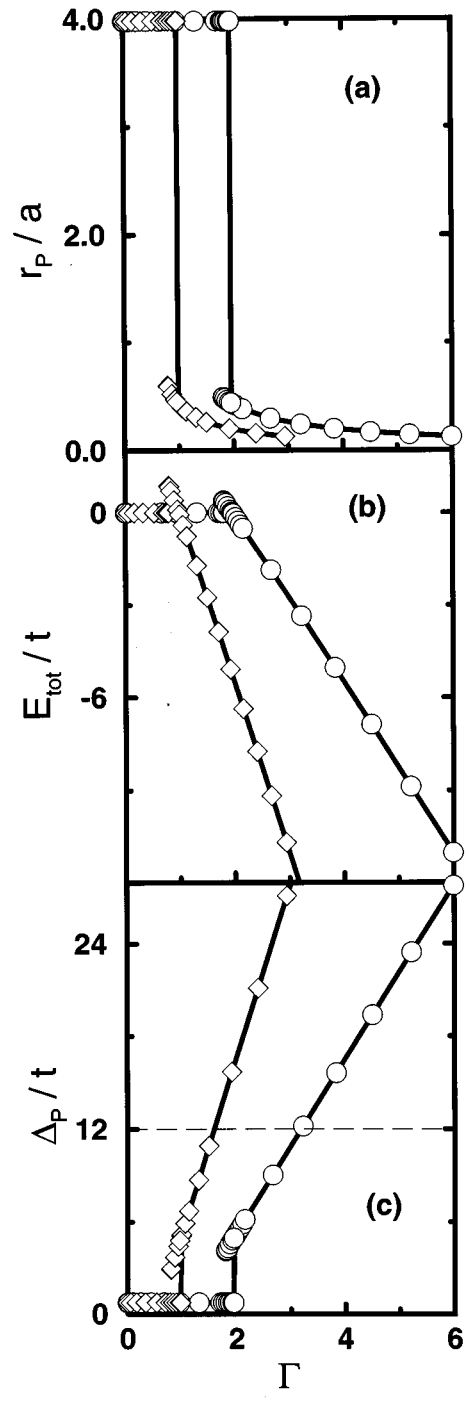


FIG. 3. Calculated properties of a polaron: (a) radius $r_P/a$, (b) total energy per electron $E_{\rm tot}/t$, and (c) the gap $\Delta_P=(\epsilon_1-\epsilon_2)/t$ in the electron spectrum as a function of electron-phonon coupling $\Gamma$. The circles give results for the single-electron polaron and the diamonds give the radius, half the total energy, and the electronic gap for the bipolaron. The Coulomb repulsion is omitted for the bipolaron ($U=U'=0$).

Because the small polaron is so well localized, the error in our calculation due to the finite size supercell is easy to control. To test this, we have varied the size of the supercell from a minimum of $2\times2\times2$ to maximum of $20\times21\times22$. The results are shown in Fig. 4. The polaron radius and total energy are insensitive to cluster size if the number of Bi

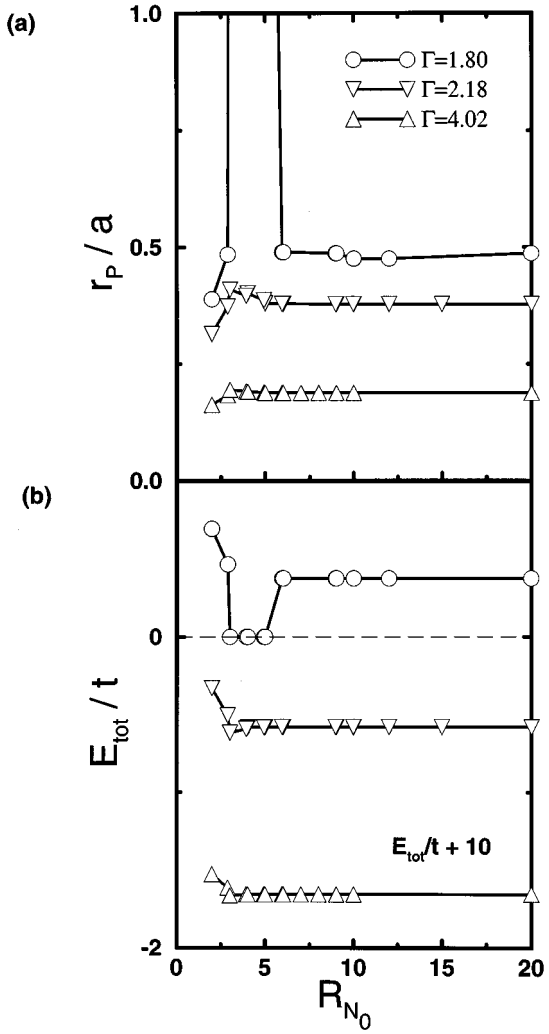


FIG. 4. Tests of finite-size errors for different values of electron-phonon coupling constants. The cluster radius is in the units of the Bi-Bi distance. The clusters used are $N_0\times N_0\times N_0$ and $(N_0-1)\times N_0\times(N_0+1)$, out to a maximum of $N_0$ of 20. The cluster radius is $R_{N_0}=N_0$ in the former case or $R_{N_0}=N_0^{1/3}(N_0^2-1)^{1/3}$ in the last case.

atoms is $\gtrsim200$. Near the transition, for cluster size not too big, the transition onset varies with cluster size. The total energy always diminishes with increase of cluster size until it becomes independent of cluster size. At $\Gamma$ far enough from the critical value the results are almost the same for all the clusters sizes. The results of Fig. 3 have no noticeable size dependence.

The nonadiabatic corrections to the large polaron energy are $0.17t$ at the transition point, which gives an unimportant correction to the critical value of $\Gamma$ (see Fig. 6). The small polaron solution is $2N$-fold degenerate: it can form at any of the $N$ Bi sites, with either spin. In this paper we ignore another nonadiabatic effect, the weak vibration-assisted tunnelling which lifts the translational degeneracy to make a narrow band with only spin degeneracy remaining.

We now compare our numerical results with analytic results obtained by a variational method introduced by Landau and Pekar (LP).[18,19] The electronic wave function is chosen to have Gaussian form

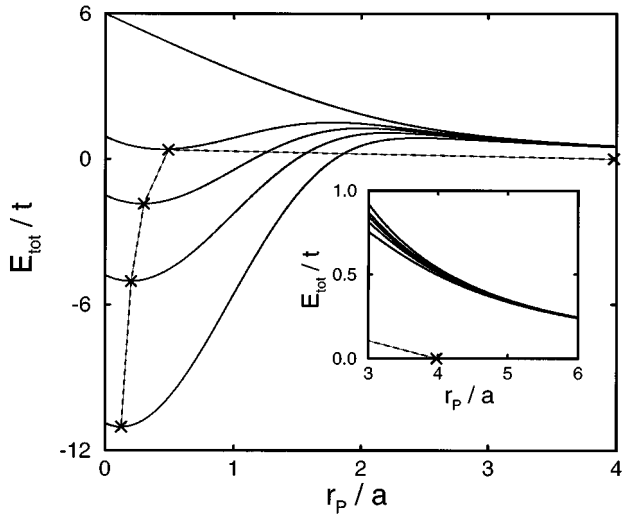


FIG. 5. Total energy *versus* polaron radius calculated in Landau-Pekar approximation for electron-phonon coupling constants $\Gamma=0$, 1.80, 2.66, 3.83, and 5.99 from top to bottom. The energy minima for $\Gamma=2.66$, 3.83, and 5.99 correspond to energies of stable localized states. The extremum at $\Gamma=1.80$ corresponds to a metastable localized state. Results from finite cluster diagonalization are shown as crosses. For numerical comparison see Table I. The inset expands the large $r_P$ part of the same curves.

$$a_i = C_0(\beta)\exp[-\beta^2(\vec{r}_i-\vec{r}_0)^2/2], \tag{15}$$

where $C_0$ is the normalization constant and $\beta$ is the variational parameter which we call the LP parameter. There are now two sequential minimizations to perform.[3] First for fixed $\beta$ the optimum displacements $\{u(\beta)\}$ are found. Then these are used to evaluate the trial total energy $E(\beta)$, and a second minimization is performed to find the optimum $\beta$. We find analytic formulas for $E(\beta)$ and the polaron radius $r_P(\beta)$:

$$E(\beta)/t = 6\left[1-q^{1/4}\frac{\theta_2(q)}{\theta_3(q)}\right]-3\Gamma\,\frac{\theta_3(q^2)^2}{\theta_3(q)^6} \times[\theta_3(q^2)-q^{1/2}\theta_2(q^2)], \tag{16}$$

TABLE I. Comparison of results obtained by the Landau-Pekar (LP) variational method and by exact diagonalization of finite clusters (cluster). The electron-phonon coupling constants are in units of bandwidth ($W=12t$). The first row in the table corresponds to the critical coupling constant at which a metastable localized state occurs. The total energies $E_{\text{total}}^{\text{LP}}$ and $E_{\text{total}}^{\text{cluster}}$ are in units of $t$. The polaron radius is given in units of the Bi-Bi distance. Cluster calculations give a slightly smaller total energy and larger radius. The phonon spectrum is perturbed by the transition from the delocalized state to localized (see text). In the LP approximation only one mode $\omega_{\text{min}}^{\text{LP}}$ changes from its initial value of $\omega_0$. In the cluster calculations, one mode $\omega_{\text{min}}^{\text{cluster}}$ is well-separated from the others.

| $g/W$ | $E_{\text{total}}^{\text{LP}}$ | $E_{\text{total}}^{\text{cluster}}$ | $r_p^{\text{LP}}$ | $r_p^{\text{cluster}}$ | $\omega_{\text{min}}^{\text{LP}}/\omega_0$ | $\omega_{\text{min}}^{\text{cluster}}/\omega_0$ |
|---|---|---|---|---|---|---|
| 2.785 | 0.398 | 0.377 | 0.448 | 0.490 | 0.824 | 0.837 |
| 3.382 | −1.848 | −1.853 | 0.290 | 0.299 | 0.925 | 0.935 |
| 4.060 | −5.040 | −5.041 | 0.198 | 0.200 | 0.965 | 0.972 |
| 5.075 | −11.03 | −11.03 | 0.126 | 0.126 | 0.986 | 0.989 |

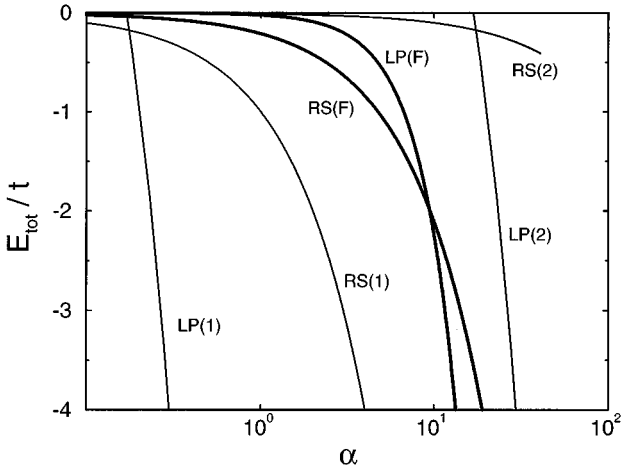


FIG. 6. Results of the Landau-Pekar (LP) variational treatment and Rayleigh-Schrödinger (RS) perturbation theory for the Fröhlich Hamiltonian (FH) and for the Rice-Sneddon model (RSM). The parameter $\alpha$ and electron-phonon coupling constant $g$ do not have a unique relation. An electrostatic model suggests the upper and lower limits on this relation which are shown for LP variational method as LP(1) and LP(2) and for RS perturbation theory as RS(1) and RS(2). Traditional results for FH are shown as LP(F) and RS(F). Note that the LP (bound state) solution for FH always exists in contrast to RSM.

$$r_P(\beta)^2 = 6q\,\theta_3'(q)/\theta_3(q), \tag{17}$$

where $q=\exp(-\beta^2)$ and $\theta_i(q)=\theta_i(0,q)$ are Jacobi's theta functions.[20] $\theta_3'(q)$ is the derivative of $\theta_3(q)$. These equations define an implicit function $E(r_P)$ which is plotted in Fig. 5 for the values $\Gamma$ equal to 0, 1.80, 2.66, 3.83, and 5.99. The crosses indicate the exact results from our finite cluster calculations. The agreement is remarkable, especially for the values of minimal total energy (see Table I). The LP solution gives a smaller value of the polaron radius. The variational solution for an infinite system agrees with the exact solution on finite clusters in finding a first-order large to small polaron transition, with no regime of intermediate polarons. Figure 5 explains the hysteresis found in the numerical results obtained by exact diagonalization. For a small range of $\Gamma$ just below the critical value the small polaron state is locally stable but separated by an energy barrier from the global (delocalized) minimum. The numerical solution follows this metastable branch until it disappears.

## IV. COMPARISON WITH FRÖHLICH POLARON

It is interesting to compare our results with the original LP treatment of the Fröhlich Hamiltonian (FH). This is shown in Fig. 6. The FH describes the coupling of an electron to a polar optical phonon of frequency $\omega_0$ (Ref. 3):

$$H_F = \sum_{i\sigma,\mathbf{q}} \hat{c}_{i\sigma}^{\dagger}\hat{c}_{i\sigma}e^{i\mathbf{q}\cdot\mathbf{R}_i}\frac{M_0}{q}[b_{\mathbf{q}}+b_{-\mathbf{q}}^{\dagger}], \tag{18}$$

where $M_0^2=4\pi\alpha\hbar(\hbar\omega_0)^{3/2}/(2m^*)^{1/2}$; the coupling constant $\alpha$ is $(e^2/\hbar)(m^*/2\hbar\omega_0)^{1/2}(\epsilon_\infty^{-1}-\epsilon_0^{-1})$ and $m^*$ is the effective mass of the electron. The FH includes long-range polar forces in a continuum approximation, in contrast to the short-range atomistic RSM of Eq. (3). The Fröhlich constant $\alpha$ is

$\approx 5.5$ for $BaBiO_3$. In this intermediate range of coupling, neither the Rayleigh-Schrödinger (RS) result $E_p=-\alpha\hbar\omega_0$ nor the Landau-Pekar (LP) result $E_p=-\alpha^2\hbar\omega_0/3\pi$ is accurate. The RS and LP energies are equal at $\alpha=3\pi$, as shown in Fig. 6.

A qualitative difference between RSM and Fröhlich polarons is that the LP bound state requires a threshold energy with RSM short-range interactions, but occurs for arbitrarily weak $\alpha$ in the FH, following the usual quantum rules for occurrence of bound states in 3D problems for short-range and long-range potentials.[11] The actual answer for the FH is believed[21] to be a continuous function of $\alpha$, whereas our treatment of the RSM gives a discontinuity. At small values of $\Gamma$, where RS perturbation theory applies, Eq. (10) gives a relatively small change in the electronic energy, but at the critical value of $\Gamma$, a sudden localization and large energy shift occur. The other qualitative difference between the RSM and Fröhlich cases is that the RSM polaron is always ''small,'' whereas the Fröhlich polaron for large $\alpha$ is ''intermediate.'' The radius of the LP bound state for the Fröhlich case is 53 Å/$\alpha$ using parameters $m^*$ and $\omega_0$ of BKBO, which is much larger than the RSM polaron. To compare quantitatively a polaron in the RSM with a Fröhlich polaron, it is necessary to have a translation between $\alpha$ and $\Gamma$. Unfortunately, this is not unique. The FH uses electrostatic couplings in a continuum approximation. Applying electrostatic ideas to the perovskite structure, one can estimate that the nearest-neighbor electron-phonon coupling $g$ should have the approximate value $4Z_+Z_-e^2/\varepsilon a$, where $Z_+e$ and $Z_-e$ are the charges on the Bi and O sites, and $\varepsilon$ is the dielectric constant. Then the same arguments which give $\alpha=5.5$ yield $\Gamma=0.65$ if we take $Z_+$ and $Z_-$ to be each 1, or $\Gamma=65$ if we take them to be 5 and 2 (e.g., $Bi^{5+}$ and $O^{2-}$). In the former case, $\alpha$ translates into $8.7\Gamma$, and in the latter case, into $0.087\Gamma$. Both translations are shown on Fig. 6. Without microscopic calculations it is impossible to say which estimate is more appropriate.

A realistic model for BKBO would need both short-range atomistic interactions and long-range polar interactions. The short-range interaction differs from the electrostatic estimate $4Z_+Z_-e^2/\epsilon a$ because of various quantum effects (electron wave functions are not point charges, and have exchange as well as electrostatic energies) which may well increase $\Gamma$ compared to electrostatic models. Experiment suggests that in an appropriate realistic model, the extreme small polaron behavior captured by the RSM dominates, at least for some materials such as BKBO in the nonmetallic range of doping, and $WO_3$ in the same range.

## V. ELECTRONIC AND VIBRATIONAL EXCITATIONS OF THE POLARON

An advantage of the exact diagonalization method is that it enables an equally good and easy calculation of electronic excitations of the Franck-Condon type where the lattice distortion is frozen in place. We simply examine the next higher-lying eigenstates without further alteration of the parameters $\{u\}$. In the range of parameter space we have explored, we have not encountered a second bound state in the polaronic well. The electronic spectrum has a gap, and the minimum energy electronic excitation is a delocalized state. The energy of this transition, denoted the ''gap'' energy, is plotted in Fig. 3(c). At the onset of polaron formation, the gap has a value $5.00t$ which increases rapidly for larger coupling constants. There is a small but noticeable finite size error in the gap calculation since the lowest electronic excited state is extended to infinity, but cut off at the supercell boundary in our work.

When a small polaron is formed, the interaction between the localized electron and the lattice vibrations can cause both a renormalization of the electron energy and of the phonon energy. Referring to Eq. (9), it is clear that the gap, or minimum value of $\epsilon_0-\epsilon_j$ in the denominator, makes a change in the electron self-energy shift relative to the one already calculated for the delocalized large polaron, probably reducing the shift because of the larger denominator (although matrix element changes need to be considered also). However, since the shift is certainly small compared to the gap itself (of order $t$), this effect can be neglected.

A more interesting effect is the change in the local vibrations near the localized electron. This problem (for intermediate polarons) was discussed by Emin.[22] If we know the one-electron energies $\epsilon_j$ and the corresponding states $|j\rangle$ at the optimal set of displacements $\{u_0\}$, then standard perturbation theory for small deviations around these displacements gives

$$\Delta\left[\frac{\partial^2 E_{\rm tot}}{\partial u_{\ell,\alpha}\partial u_{\ell',\beta}}\right]=\sum_j \frac{\langle 0|V_{\ell,\alpha}|j\rangle\langle j|V_{\ell',\beta}|0\rangle}{\epsilon_0-\epsilon_j}, \quad (19)$$

$$V_{\ell,\alpha}=\frac{\partial H_{e\text{-ph}}}{\partial u_{\ell,\alpha}}.$$

This equation omits terms containing second derivatives of $H$ because they are consistently omitted in our model.

The LP approximation gives a particularly simple solution to this problem. Since we do not have a complete set of states in this approach, instead, we find the energy as a general function of the displacements $\{u_0\}$ and the LP parameter $\beta$:

$$E(\vec{u},\beta)=\frac{1}{2}\vec{u}^{\dagger}\cdot\hat{A}\cdot\vec{u}+\vec{L}^{\dagger}(\beta)\cdot\vec{u}+f(\beta), \quad (20)$$

where $\vec{u}$ is the $3N$-vector displacement, $\hat{A}$ is the bare force constant matrix (which is a constant times the unit matrix in our model), $\vec{L}$ is the force on the atoms caused by the localized electron, and $f$ is the localized electron hopping energy. Expressions for $\vec{L}$ and $f$ are easy to derive. Straightforward linear algebra leads to expressions for the optimum values $\{u_0\}$ and $\beta_0$. We then Taylor expand Eq. (20) to second order for small deviations $\{\delta u\}$ and $\delta\beta$ around the optimum values. Finally, for fixed deviations $\{\delta u\}$ the optimum value of $\delta\beta$ is found. Inserting this into the Taylor expansion, the modified force constant matrix $\hat{A}+\delta\hat{A}$ is found:

$$\delta\hat{A}=-\frac{\vec{L}'\vec{L}'^{\dagger}}{f''-\vec{L}^{\dagger}\cdot\hat{A}^{-1}\cdot\vec{L}''}, \quad (21)$$

with $\delta\hat{A}<0$ as the result of stability condition. The primes on the right-hand side of Eq. (21) denote derivatives by $\beta$.

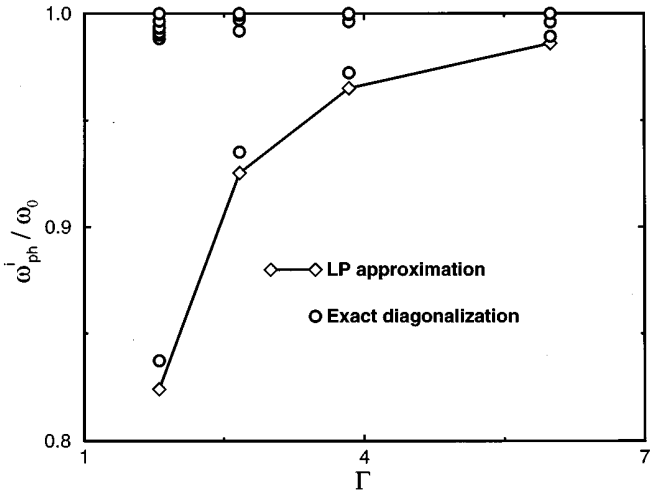


FIG. 7. Phonon frequency shifts $\omega^i_{\rm ph}/\omega_0$, at coupling constants $\Gamma=1.80$, 2.66, 3.83, and 5.99 for cluster size $5\times6\times7$. The phonon modes (circles) are distributed from $\omega_{\rm min}$ to $\omega_0$, the first being well separated from others. Results from the Landau-Pekar approximation are shown by diamonds.

Note that the alteration of the force constant matrix in the LP approximation is factorizable, and since $\hat{A}$ is proportional to the unit matrix, only one eigenvalue is altered, the corresponding eigenvector being proportional to $\vec{L}'$. The static displacements $\{u_0\}$ in the LP approximation are given by $-\hat{A}^{-1}\vec{L}(\beta_0)$. Thus in the LP approximation, one vibrational eigenvector splits off from the degenerate frequency $\omega_0$, shifting to lower energy, and having an eigenvector proportional to the derivative of the static displacements by the LP parameter $\beta$. The symmetry of this mode is identical to the symmetry of the static displacement.

We have also made an exact calculation of the modified vibrational spectrum using finite clusters, and the answers, shown in Fig. 7, and also in Table I, agree nicely with the LP approximation, but in addition to the one strongly altered frequency, a few other frequencies are pulled weakly below the unperturbed frequency $\omega_0$. Our results are consistent with Emin's.[22]

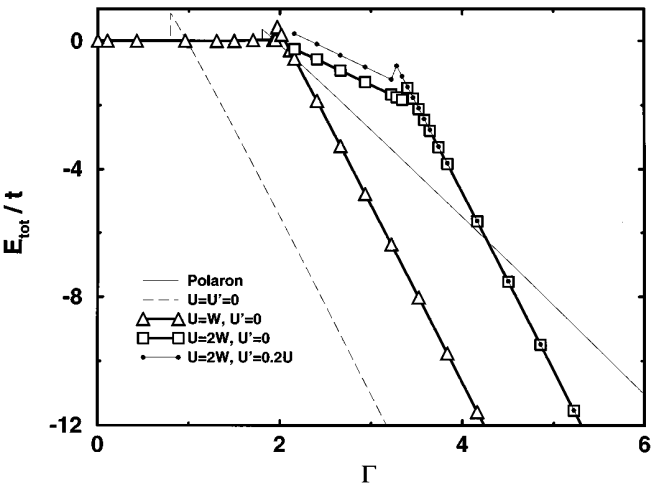


FIG. 8. Total energy (per electron) of the bipolaron for different values of Coulomb repulsion. The supercell size is $5\times6\times7$. At $U=2W$ for $\Gamma$ between 1.97 and 3.40, the total energy corresponds to two small polarons separated as far as possible in the cell; because the cell is not infinitely large, there is Coulomb repulsion which raises the energy above the isolated polaron energy shown as the thin curve (identical to Fig. 3).

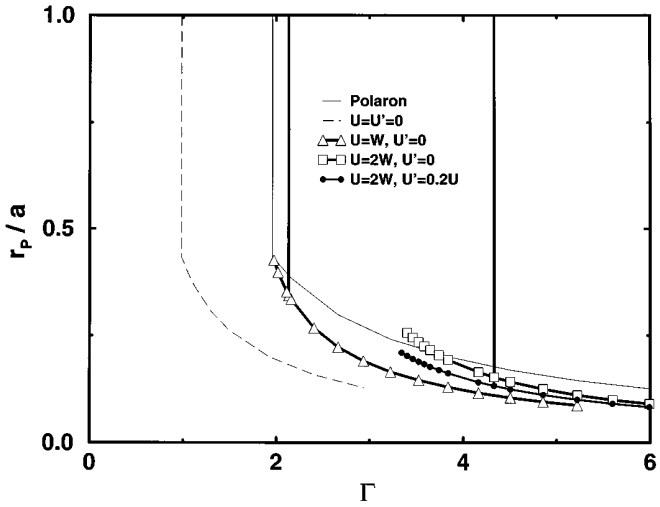


FIG. 9. Bipolaron radius as a function of $\Gamma$ for different values of Coulomb repulsion. Vertical lines indicate stability limits where bipolarons (with $U\lesssim W$) decay into isolated small polarons or into isolated large polarons when $U\gtrsim W$. At $\Gamma$ less than the stability point, radii of metastable bipolaron states are shown. The domain of metastability is artificially enhanced by finite size effects.

Thus we expect that a characteristic signature of the small polaron state should be a localized vibrational mode whose symmetry copies that of the polaronic distortion, that is, the symmetry is the same as the point symmetry in the crystal of the ion on which the polaron is centered (full cubic symmetry $A_1$ in our case). Such modes might be measurable by Raman scattering using a laser which is resonant with an electronic transition of the polaron. Also they might appear as side bands on the electronic polaron absorption spectrum.

## VI. BIPOLARON

We now ask what happens in our model when a second electron is added. If we neglect the Coulomb interaction, the

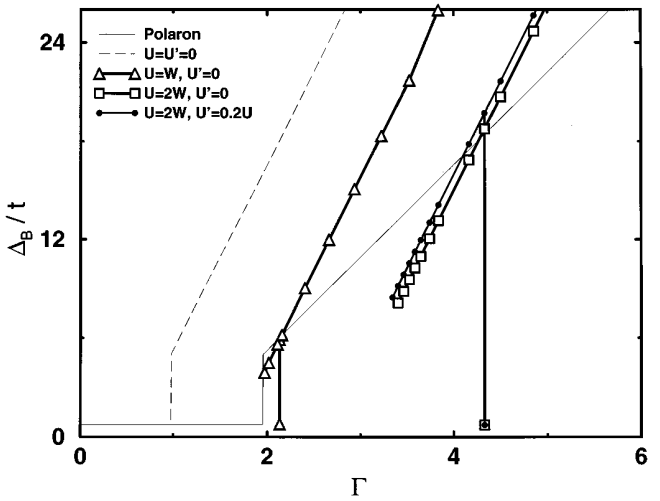


FIG. 10. The gap in the electron spectrum as a function of $\Gamma$. Due to the finite size of the cluster the gap is finite even in the delocalized state.

answer is that two spatially separated polarons are unstable relative to the formation of a singlet bipolaron state in which both electrons are on the same site. If we allow no further lattice relaxation beyond the single electron polaron, then the energy of the bipolaron is already lower than two separated polarons because the (negative) electronic eigenvalue is doubled but the positive lattice strain energy is unchanged; additional lattice relaxation will occur only if it lowers the energy, and since there are now two electrons exerting each force $g$ on the neighboring oxygens, there will be additional relaxation. Results are shown in Fig. 3, where we plot the total energy per electron. The critical coupling for bipolaron formation is $\Gamma_B = 0.99$, significantly less than for polaron formation which starts at $\Gamma_P = 1.96$. At onset of bipolaron formation, the radius and the electronic gap (0.44$a$ and 5.00 $t$, respectively) are approximately the same as for polaron formation at its onset, but at equal values of $\Gamma$ the bipolaron is smaller and has a larger gap.

Of course it is unrealistic to ignore the Coulomb repulsion which will act in the direction of destabilizing the bipolaron. Our model permits us to make exact (finite size) calculations for the bipolaron by solving the appropriate two-particle equation, that is, finding the exact two-particle wave function

$$\Psi(\{u\}) = \sum_{i,j} a_{i,j}(\{u\}) c^{\dagger}_{i,\uparrow} c^{\dagger}_{j,\downarrow} |\mathrm{vac}\rangle. \tag{22}$$

This calculation is of course far more demanding than the corresponding polaron case, Eq. (6), because it requires on each step of the minimization procedure finding the smallest eigenvalues of a $N^2 \times N^2$ matrix rather than a $N \times N$ matrix. A Lanzcos algorithm has allowed us to calculate for $N$ as large as $5 \times 6 \times 7$. Because the bipolaron turns out to be again well localized, the finite system size does not cause a noticeable error. Also for the same reason, the long-range Coulomb repulsion is not very important. The results are shown in Figs. 8–10. Our result agrees with Emin and Hillery's variational analysis[23] that for short-range electron-phonon interaction the only possible three-dimensional bipolaron states are small bipolarons.

An interesting feature shown in Fig. 10 is that the gap is larger at the onset of bipolaron formation in the presence of the long-range Coulomb repulsion, presumably due to stronger localization of electrons. At fixed $\Gamma$ the Coulomb forces reduce the gap with increasing $U$.[24]

## VII. SUMMARY

Bipolaron formation is strongly affected by Coulomb forces in a cubic perovskite lattice. Due to Coulomb repulsion between two electrons localized on the same site the onset of bipolaron formation can be postponed and polaron states are energetically favorable. The polarons and bipolarons formed in this lattice are small and exist only above some critical value of electron-phonon coupling. The transition from delocalized to localized polaron state is discontinuous, with no intermediate-size solution. This jump is not caused by finite-size errors and is present also in variational calculations using Landau-Pekar approximation. The total energy has hysteretic behavior with metastable states occurring near the critical coupling constant. These metastable states could in principal be observed, for example, by tuning the coupling constant with applied pressure. A gap opens in the electron spectrum at the transition from delocalized to localized polaron states, and new localized vibrational states occur with energies decreased below those of the undoped host.

## ACKNOWLEDGMENTS

We thank V. Emery, D. Emin, and S. J. Miyake for useful discussions and comments. This work has supported by NSF Grant No. DMR 9417755.

[1] The idea of a self-trapped electron in a NaCl lattice was first introduced by L. D. Landau, Phys. Z. Sowjetunion **3**, 664 (1933).

[2] A. S. Alexandrov and N. F. Mott, *Polarons and Bipolarons* (World Scientific, Singapore, 1995).

[3] G. D. Mahan, *Many-Particle Physics* (Plenum, New York, 1990).

[4] J. Appel, in *Solid State Physics*, edited by F. Seitz, D. Turnbull, and H. Ehrenreich (Academic, New York, 1968), Vol. 21, p. 193.

[5] J. T. Devreese, in *Encyclopedia of Applied Physics*, edited by G. L. Trigg (VCH, New York, 1996), Vol. 14, p. 383.

[6] N. F. Mott, *Metal-Insulator Transitions*, 2nd ed. (Taylor & Francis, London, 1990).

[7] Although the neutron powder diffraction experiments [see D. E. Cox and A. W. Sleight, Solid State Commun. **19**, 969 (1976) for $BaBiO_3$ and S. Pei *et al.*, Phys. Rev. B **41**, 4126 (1990) for $Ba_{1-x}K_xBiO_3$] indicated $BiO_6$ octahedral tilting as well as symmetric oxygen breathing-mode distortions, we consider only the latter responsible for polaron/bipolaron formation.

[8] T. M. Rice and L. Sneddon, Phys. Rev. Lett. **47**, 689 (1981).

[9] V. N. Kostur and P. B. Allen (unpublished).

[10] Y. Toyozawa, Prog. Theor. Phys. **26**, 29 (1961).

[11] D. Emin and T. Holstein, Phys. Rev. Lett. **36**, 323 (1976).

[12] L. F. Mattheiss and D. R. Hamann, Phys. Rev. Lett. **60**, 2681 (1988).

[13] W. D. Mosley *et al.*, Phys. Rev. Lett. **73**, 1271 (1994).

[14] W. Reichardt and W. Weber, Jpn. J. Appl. Phys. **26**, Suppl. 26-3, 1121 (1987); C.-K. Loong *et al.*, Phys. Rev. Lett. **62**, 2628 (1989).

[15] J. Yu, X. Y. Chen, and W. P. Su, Phys. Rev. B **41**, 344 (1990).

[16] P. Prelovšek, T. M. Rice, and F. C. Zhang, J. Phys. C **20**, L229 (1987).

[17] J. K. Cullum and R. A. Willoughby, *Lanczos Algorithms for Large Symmetric Eigenvalue Computations* (Birkhäuser, Boston, 1985), Vol. 1-2.

[18] S. I. Pekar, Zh. Eksp. Teor. Fiz. **16**, 341 (1946); **16**, 375 (1946); **16**, 433 (1946); L. P. Landau and S. I. Pekar, *ibid.* **18**, 419 (1948); see also S. I. Pekar (unpublished).

[19] S. J. Miyake, J. Phys. Soc. Jpn. **41**, 747 (1976).

[20] *Handbook of Mathematical Functions*, edited by M. Abramowitz

and I. A. Stegun (Dover, New York, 1972).
[21] P. Sheng and J. D. Dow, Phys. Rev. B **4**, 1343 (1971).
[22] D. Emin, Phys. Rev. B **43**, 8610 (1991).
[23] D. Emin and M. S. Hillery, Phys. Rev. B **39**, 6575 (1989).

[24] It is interesting to note that in the zero-radius approximation which corresponds to (bi)polaron 100% localized on one site, the stability points for polaron and bipolaron coincide at $U=W$.